Journal of Southeast University (English Edition) Vol. 25, No. 3, pp. 408 – 412 Sept. 2009 ISSN 1003—7985

Structure and magnetic properties of Zn ferrite nanoparticles

Zhang Yi Wang Kai Ren Zhiyan Zhai Ya

(Department of Physics, Southeast University, Nanjing 211189, China)

Abstract: A series of $Zn_xFe_{3-x}O_4$ ($x = 0$, 0.15, 0.30, 0.40, 0.48, 0.60, 0.70) nanoparticles prepared by hydrothermal method are studied by use of transmission electron microscope, X-ray diffraction, vibrating sample magnetometer, superconducting quantum interference device magnetometer and Mössbauer spectrometer. All samples present a spinel structure. The lattice constant increases with the increase in the Zn content while the grain size decreases from 18 nm to 9 nm. Moreover, the saturation magnetization at 5 K and 293 K increases initially when $x \leqslant 0.40$ and subsequently decreases when $x > 0.40$. At room temperature, Mössbauer spectra exhibit a change from a well-defined sextet spectrum to a doublet spectrum as the Zn content increases. The doublet spectrum begins to appear when $x = 0.6$, while it begins when $x = 0.80$ for the bulk materials. The results of magnetization and Curie temperature measurements indicate that the doublet spectrum is due to the surperparamagnetic state of the nanoparticles. Furthermore, the relationship between the hyperfine field variation and the cation distribution is discussed. The variation of magnetic properties is interpreted by the three-sublattice Yafet-Kittel (Y-K) model.

Key words: magnetic materials; Zn ferrite; Mössbauer spectra; magnetic properties

Magnetic nanoparticles have attracted much interest in recent years. It is attributed not only to their wide potential applications in magnetic fluids, information storage media, thermochemotherapy of tumors, etc.[1-3], but also to a fundamental perspective. Nanoparticles of ferrites with the spinel structure have been found to show different properties from those in bulk state due to their reduced dimensions[4], which is important to be examined. Various bulk Zn-substituted ferrites[5] which were well studied have been commercial products for a long time, since their Curie temperature, saturation magnetization, magnetic susceptibility etc. can be adjusted by the zinc content. These properties are primarily related to the cation distribution and the spin alignment in sublattices[6]. It is an interesting topic to study the relationship between the properties of Zn-substituted ferrite nanoparticles and the cation distribution. Zn-substituted ferrite can be denoted as $(Zn_x^{2+}Fe_{1-x}^{3+})[Fe_{1+x}^{3+}Fe_{1-x}^{2+}]O_4$, where the parentheses and the square brackets refer to cations occupying tetrahedral sites and octahedral sites, respectively. The information of the cation distribution can be obtained by X-ray diffraction (XRD)[7], neutron diffraction[8] and Mössbauer spectrometer[9].

In this paper, $Zn_xFe_{3-x}O_4$ nanoparticles prepared by the hydrothermal method are studied. By comparing the magnetization and the ordering behaviors of the nanoparticles with those in the bulk materials, the magnetic properties affected by the structure and the size effects of the nanoparticles are measured and discussed.

1 Experiments

All the samples were prepared by the hydrothermal method[10]. Ferric chlorides, zinc chlorides and ferrous sulfate were dissolved in distilled water according to stoichiometric ratios. By dropping the solution of NH_4OH slowly into the above mixed solution, $Zn_xFe_{3-x}O_4$ nanoparticles were formed by co-precipitation. The reaction was carried out under hydrothermal conditions. During the reaction process, the pH was kept at 9 to 11. The precipitates were filtered and washed several times with deoxied distilled water, and finally dried at room temperature under nitrogen protection. The reaction involved in this process can be represented as

$$xZn^{2+} + (1-x)Fe^{2+} + 2Fe^{3+} + 8OH^- = Zn_xFe_{3-x}O_4 + 4H_2O$$

The X-ray diffraction (XRD) measurement was performed by an ARL X'TRA diffractometer using Cu Kα radiation. The chemical composition of the particles was confirmed by EDX analysis with scanning electron microscopy (FEI Company). The morphologies of the products were observed by a JEM-2000EX (JEOL) transmission electron microscopy (TEM) at 120 kV. The magnetic properties of the samples were measured with a vibrating sample magnetometer (VSM, Lakeshore, model 7300). The Mössbauer spectra (MS) for various samples were measured with a radioactive source of ^{57}Co in a Rh matrix at room temperature in a transmission configuration and in the mode of constant acceleration. The spectrometer was calibrated using the room temperature spectrum of an α-Fe foil. Zero-field-cooled (ZFC) and field-cooled (FC) curves were measured between 5 K and 300 K by the SQUID magnetometer (quantum design). The value of the cooling field was about 100 Oe.

2 Results and Discussions

As presented in Fig. 1, the TEM image for $Zn_xFe_{3-x}O_4$ ($x = 0.40$) nanoparticles shows that they are homogeneous particles with nearly spherical shapes and do not exhibit a solvent or organic surface. The surface ratio of Zn to Fe obtained by the EDS is basically consistent with the value we designed. The diameters of the nanoparticles are counted according to the TEM images, and the results indicate that all of the samples exhibit a narrow size distribution. The structural information from a single $Zn_xFe_{3-x}O_4$ nanoparticle is also obtained by using a high resolution TEM, which shows

Received 2009-05-26.

Biographies: Zhang Yi (1980—), male, graduate; Zhai Ya (corresponding author), female, doctor, professor, yazhai@seu.edu.cn.

Foundation items: The National Natural Science Foundation of China (No. 50871029), Open Foundation of National Laboratory of Solid State Microstructure of Nanjing University, Open Foundation of Key Laboratory of the Thin Film Material of Jiangsu Province, the Science Research Foundation of Graduate School of Southeast University, the Jiangsu Provincial Innovation Project.

Citation: Zhang Yi, Wang Kai, Ren Zhiyan, et al. Structure and magnetic properties of Zn ferrite nanoparticles[J]. Journal of Southeast University (English Edition), 2009, 25(3): 408 – 412.

that the products are all single crystal, as shown in the inset of Fig. 1. The inset is a high resolution TEM image of a single particle.

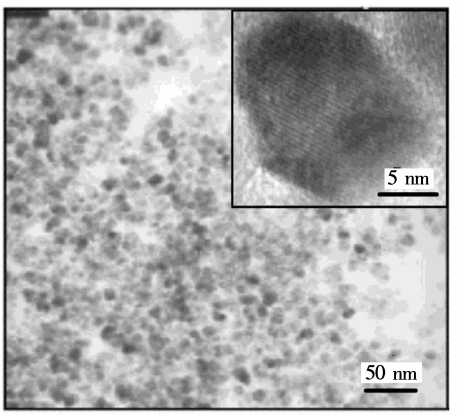

Fig. 1 The TEM images of $Zn_{0.4}Fe_{2.6}O_4$ nanoparticles

The X-ray diffraction patterns of the $Zn_xFe_{3-x}O_4$ nanoparticles are shown in Fig. 2. The observed diffraction lines are found to be similar to the standard spectrum of Fe_3O_4 ($x = 0$)

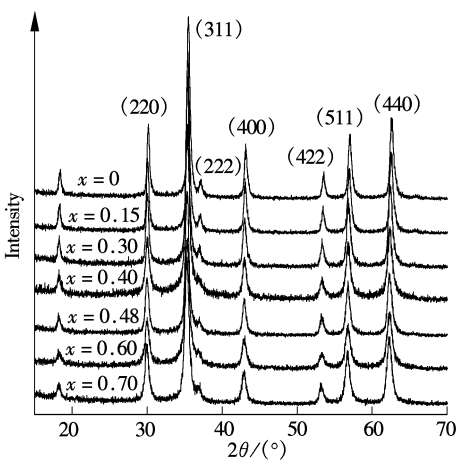

Fig. 2 XRD analysis for $Zn_xFe_{3-x}O_4$ nanoparticles with various Zn contents

without extra lines, indicating that the product possesses a single phase of the cubic spinel structure and no unreacted phase exists. According to the Bragg formula $2d\sin\theta = \lambda$, the average lattice constant increases from 0.839 0 to 0.843 3 nm with the increase of the zinc substitution as shown in Fig. 3 (a) due to the substitution of Zn^{2+} ions (0.074 nm) for Fe^{3+} ions (0.060 nm) at site A. The average particle size can be estimated according to the diffraction peaks by using the Scherrer formula, without considering possible contributions of crystal stress; i. e. ,

$$D = \frac{k\lambda}{\beta\cos\theta}$$

where D is the average diameter of the particles; λ = 0.154 18 nm is the wavelength of the X-ray; β is the line width at half height of the peak; θ is the diffractive angle and k is a constant. The estimated particle size decreases from 18 to 9 nm with the increase in the Zn content, which agrees with the TEM data as shown in Fig. 3(b).

The Mössbauer spectra at room temperature for the $Zn_xFe_{3-x}O_4$ nanoparticles are shown in Fig. 4. When x increases to 0.6, the spectra change from a well defined sextet spectrum to a doublet spectrum. The MS spectra of the bulk $Zn_xFe_{3-x}O_4$ in Ref. [11] obviously exhibit similar variations due to the occurrence of paramagnetic states when the Curie temperature decreases to room temperature or even lower due to the reduced A-B exchange interaction caused by high Zn content. However, in our experiments, with the increase in the Zn content and the decrease in the particle size, the thermal relaxation effects on the intensity and shape of the spectra are clearly observed when x = 0.30,

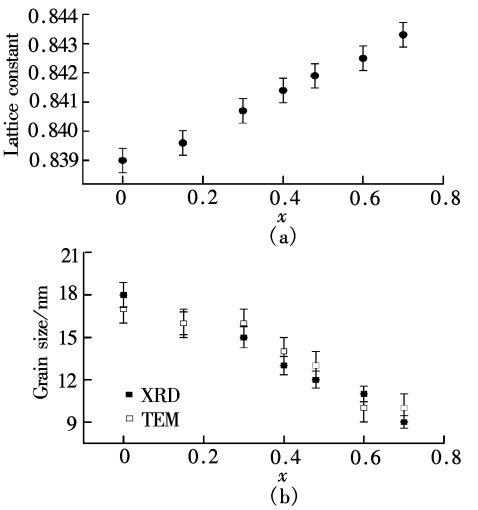

Fig. 3 The lattice constant and average grain size vs. Zn content. (a) The lattice constant changes with various Zn contents; (b) The average grain size changes with various Zn contents

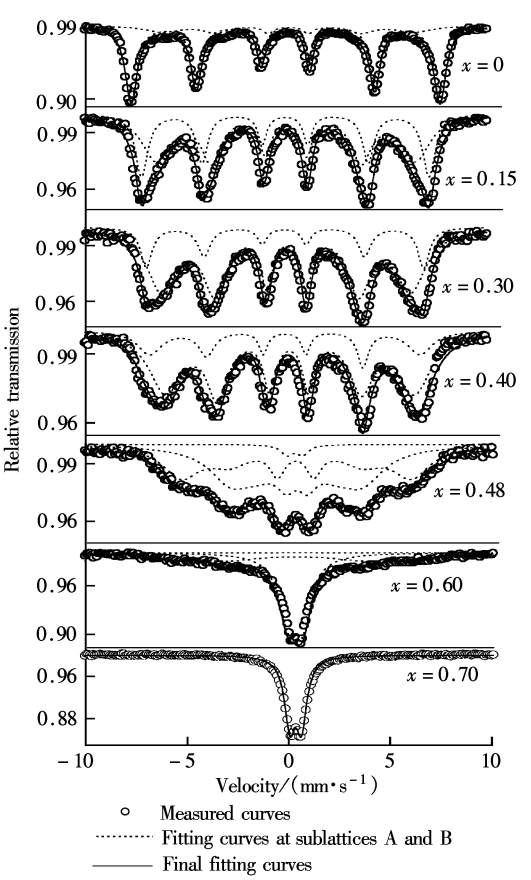

Fig. 4 The Mössbauer spectra of the $Zn_xFe_{3-x}O_4$ nanoparticles with various Zn contents at room temperature

0.40, 0.48. Furthermore, the doublet spectrum begins to appear when $x = 0.60$, while it starts when $x = 0.80$ for the bulk materials, which might be attributable to a superparamagnetic behavior. The XRD measurement results indicate that the grain size decreases to about 10 nm when $x = 0.60$. Therefore, the doublet spectrum at room temperature may be attributable to the superparamagnetic relaxation effects in the nanosized grains.

The measured spectra are fitted by using two sets of magnetic sextet spectra corresponding to Fe^{3+} ions at site A and (Fe^{2+}, Fe^{3+}) ions at site B and one set of doublet spectrum corresponding to the supermagnetic or paramagnetic phase. The fitted sub-spectra are displayed with dotted lines as shown in Fig. 4. The circles stand for the measured spectra and the solid lines represent the final fitting curves which fit the measured spectra well. The refined values of the hyperfine interactions parameters are given in Tab. 1. The values of isomer shifts (IS) and quadrupole shifts (QS) of Zn ferrite nanoparticles at room temperature for sites A and B have minor differences from those of the bulk materials[11]. The hyperfine magnetic field(HMF) of these nanoparticles shares the same changing tendency as that of the bulk materials. The HMF of site A is greater than that of site B, all of which are reduced with the increase in the Zn content, as shown in Tab. 1. The reduction of the hyperfine magnetic field may be attributable to the following two reasons.

Tab. 1 Hyperfine interactions parameters extracted from Mössbauer spectra at 293 K

x	Site	IS/ (mm·s^{-1}) ($\delta = 0.06$)	QS/ (mm·s^{-1}) ($\delta = 0.03$)	HMF/T ($\delta = 0.2$)	Relative area/% ($\delta = 2$)
0	A	0.33	0.01	49.7	60
	B	0.39	0.02	42.5	40
0.15	A	0.34	0.02	46.3	58
	B	0.36	0.01	41.5	42
0.30	A	0.28	0.03	44.6	57
	B	0.38	−0.02	40.0	43
0.40	A	0.29	0.01	43.5	56
	B	0.45	0.02	40.0	44
0.48	A	0.36	0.01	36.9	36
	B	0.37	0.01	30.5	40
		0.29	0.74		24
0.60		0.36	0.52		78
	B	0.38	0.05	24.3	22
0.70		0.35	0.57		100

Note: δ denotes uncertainty of the corresponding parameters.

First, the magnetic coupling should become weak when Fe ions are gradually substituted by non-magnetic Zn ions. This can be confirmed by the results of EXAFS in our former work[12]. Fig. 5 shows the relationship between the distribution of Zn ions and the hyperfine magnetic field change of sites A and B as a result of the increase of the Zn concentration. The results indicate that the hyperfine magnetic field is related to the cation distribution and the superexchange interactions. There are three kinds of exchange interactions in the sublattices A and B of the spinel structure of ferrite, which can be represented as A-O-B, A-O-A, and B-O-B. The A-O-B exchange interaction is known to be much greater than the A-O-A and B-O-B exchange interactions. The Zn ions preferentially occupy site A at low Zn doping. The fitted results of EXAFS indicate that when $x < 0.40$, the dopant of Zn ions almost totally occupy site A while the molar percentage of Zn^{2+} in the total ions at site B is below 5%. The diamagnetic Zn ions at site A result in a breaking of nearest-neighbor interaction. They also weaken the superexchange of Fe-O-Fe between sites A and B and thus decrease the hyperfine magnetic fields of both the sites. As shown in Fig. 5, when $x > 0.40$, the percentage of Zn ions at site B increases dramatically while that at site A increases slightly with the increase in the Zn content. The more Zn ions substituting Fe ions in sublattices A and B, the more nearest-neighbor interactions are broken. The dominant A-O-B interaction decreases rapidly, which makes the hyperfine magnetic fields of both sites decrease sharply and even results in the disappearance of the hyperfine magnetic field when $x > 0.60$.

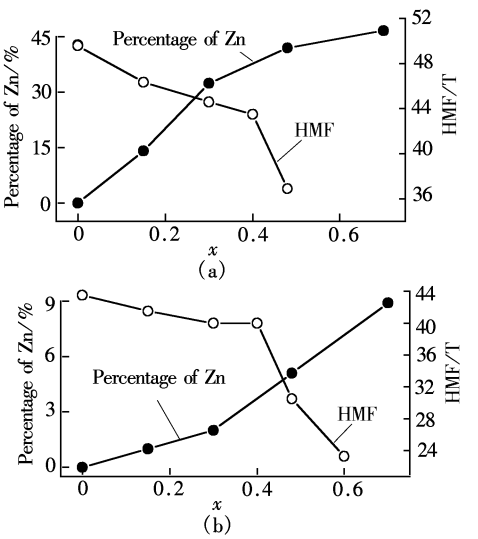

Fig. 5 The dependence of Zn ion distributions and HMF on Zn concentration for $Zn_xFe_{3-x}O_4$. (a) Site A; (b) Site B

Secondly, the grain size of the particles decreases with the increase in the Zn content, which results in a relatively stronger collective magnetic excitation and thermal disturbance effect. And it also reduces the superexchange interactions in the nanoparticles. The relative area of the Mössbauer doublet sub-spectrum, as shown in Tab. 1, sharply increases from 24% to 78% as the Zn content increases from 0.48 to 0.6, indicating that the superparamagnetic phase increases quickly. This can be confirmed by the temperature dependence of the magnetic hysteresis loop.

The temperature dependence of the saturation magnetization M_s of the $Zn_xFe_{3-x}O_4$ nanoparticles is shown in Fig. 6. Obviously, the Curie temperature T_c drops with the increase in the substitution of Zn^{2+} ions for Fe^{3+} ions. The relationship between T_c and the Zn content x is nearly linear, which agrees with that of the bulk materials[13]. The Curie temperature drops from 840 to 453 K with the increase in x from 0 to 0.70. It should be noted that the Curie temperature is still above room temperature when $x = 0.70$, implying that the doublet spectrum in the Mössbauer spectrum should not result from the paramagnetic phase.

Fig. 7 shows the hysteresis loop of the sample when $x = 0.40$, which is measured by VSM and SQUID at 293 K and 5 K. It can be seen that the saturation magnetization and the coercive field at 293 K are much less than those at 5 K, implying the significant superparamagnetic effect on the room temperature magnetic properties. The coercivity of the $Zn_{0.4}Fe_{2.6}O_4$ nanoparticles at 5 K increases significantly to 255 Oe, which is much greater than 13 Oe at 293 K. The

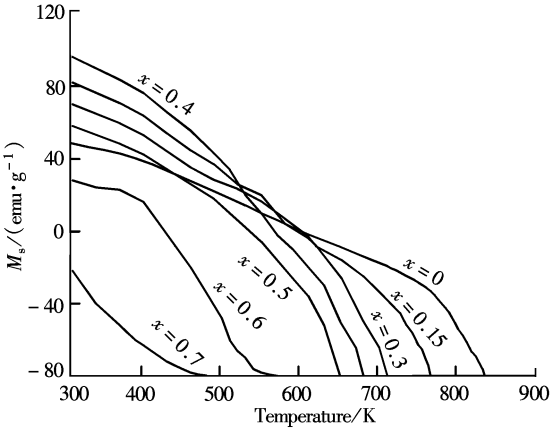

Fig. 6 The temperature dependence of the magnetization of the $Zn_xFe_{3-x}O_4$ nanoparticles at H = 5 000 Oe

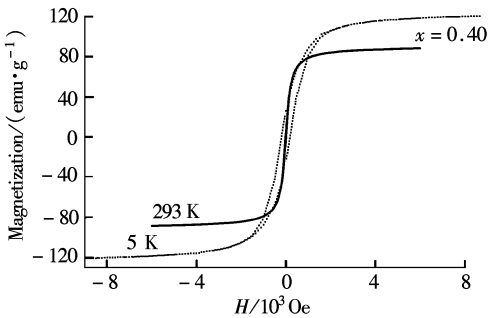

Fig. 7 The hysteresis loop of the $Zn_{0.4}Fe_{2.6}O_4$ nanoparticles measured by SQUID at 5 K and by VSM at 293 K

saturation magnetization also shows an obvious increase from 88 emu/g at 293 K to 123 emu/g at 5 K. Similar phenomena occur for all of the samples. The magnetization and the coercivity at 5 K and 293 K exhibit a strong dependence on the temperature for the $Zn_xFe_{3-x}O_4$ nanoparticles. The difference between high and low temperature are found to be associated with the grain size. When the grain size becomes smaller, the magnetization and the coercivity show a greater change, which validates the results of the Mössbauer spectra. The low temperature dependence of the magnetization for various Zn contents is also measured by SQUID for both the zero-field-cooled(ZFC) and the field-cooled(FC) under a field of 100 Oe from 300 to 5 K. The blocking temperature T_b is found to decrease as x increases from 0 to 0.70. Fig. 8 shows that for the $Zn_xFe_{3-x}O_4$ nanoparticles, T_b = 280, 150, and 70 K correspond to x = 0.48, 0.60 and 0.70, respectively. They are much lower than the corresponding Curie temperatures, indicating that T_b can be the blocking temperature of certain superparamagnetic nanoparticles. Therefore, although the large difference in characteristic time in the SQUID magnetometry and some difference in T_b caused by the MS measurement, the doublet spectrum in the Mössbauer spectra can be attributed in part to superparamagnetic particles in the sample when the Zn content is less than 0.70[14].

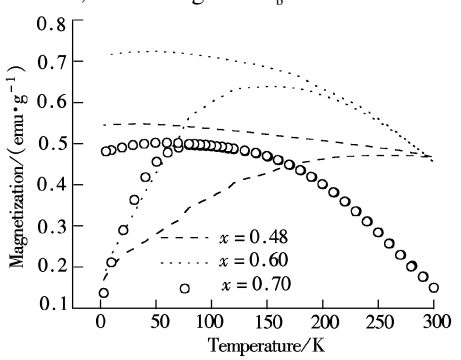

Fig. 8 The temperature dependence of FC and ZFC for the $Zn_xFe_{3-x}O_4$ nanoparticles under a field of 100 Oe

As shown in Fig. 9(a), with the increase in the Zn content, the M_s at 293 K increases when $x \leqslant 0.4$ and decreases when $x > 0.4$, illustrating a changing tendency similar to that of the bulk system of $Zn_xFe_{3-x}O_4$ and other mixed ferrites[13]. However, the saturation magnetization of the $Zn_xFe_{3-x}O_4$ nanoparticles is smaller than that of the bulk materials, and the maximum of M_s appears when x = 0.4, which is higher than 0.3 reported in Ref. [13]. The variations in M_s of the nanoparticles can be explained by cation distribution and superexchange interaction[15]. As the Zn content is small, nonmagnetic Zn cations substituting Fe cations at site A can reduce the magnetic moment in sublattice A and increase the differences of the magnetic moments between sublattices A and B, which make the total magnetization increase. Supposing that the magnetic moment of Fe cations at site B is antiparallel to that at site A due to the dominant superexchange interaction(A-O-B) between sublattices A and B, the magnetic moment μ per formula of the system can be estimated by $(4+6x)\mu_B$ on the basis of the Neel model of the spin-only moment, where the magnetic moments of Fe^{3+} and Fe^{2+} ions in Bohr magnetons μ_B are five and four, respectively. For the high Zn content, the decrease in the total magnetization of the products obtained

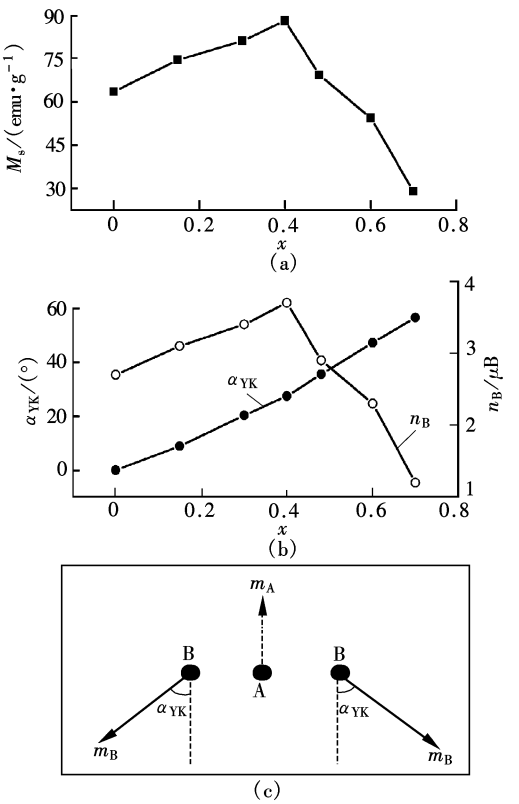

Fig. 9 The measured and calculated magnetic parameters of $Zn_xFe_{3-x}O_4$ nanoparticles. (a) Measured values of M_s as a function of Zn content at 293 K; (b) Calculated values of saturation magnetization n_B and Yafet-Kittel angle α_{YK} as a function of Zn content; (c) Schematic plot of Yafet-Kittel model

by the VSM measurement can be explained by the model of the noncollinear spin arrangement. According to the Yafet-Kittel three-sublattice model with noncollinear spin arrangement, the saturation magnetization of the Zn ferrite nanoparticles with various Zn contents can be calculated, as shown in Fig. 9(b). The detailed calculation process can be found in our previous work[12]. α_{YK} is the slant angle between the magnetic moments in sublattices A and B in the Yafet-Kittel model. With the increase in x, the calculated values increase initially and then decrease, reproducing the results of the hysteresis loop measurement with the maximum value of magnetic moment at $x = 0.4$.

3 Conclusion

A series of Zn ferrite nanoparticles with spherical shape are prepared by hydrothermal method. The hysteresis loop of the $Zn_xFe_{3-x}O_4$ particles are measured by VSM and SQUID at 293 K and 5 K. The results indicate that the samples exhibit a strong dependence of the saturation magnetization on the composition and the temperature. With the increase in the Zn content, the saturation magnetization increases initially when $x \leqslant 0.4$ and subsequently decreases, showing a changing tendency similar to that of the bulk Zn ferrites. The magnetization and the coercivity increase with the decrease in the temperature. The Mössbauer spectra of the $Zn_xFe_{3-x}O_4$ nanoparticles obtained at room temperature display a doublet spectrum when $x = 0.60$. According to the results of XRD and systematic magnetic measurements, we infer that the doublet spectrum of the Mössbauer spectra results from the superparamagnetism of part particles of the samples at room temperature when $x = 0.60$. The hyperfine magnetic field at the tetrahedral sites is larger than that at the octahedral sites, both of which decrease with the increase in the Zn content. The reduction of the hyperfine field is attributable to the nonmagnetic Zn ions substituting Fe ions and the corresponding decrease in the grain size of the particles.

References

[1] Suto M, Kosukegawa H, Maruta K, et al. Heat diffusion characteristics of magnetite nanoparticles dispersed hydro-gel in alternating magnetic field [J]. *J Magn Magn Mater*, 2009, **321**(20): 3483 - 3487.

[2] Lebedev A V, Lysenko S N. A multifunctional stabilizer of magnetic fluids [J]. *Appl Phys Lett*, 2009, **95**(1): 135081 - 135083.

[3] Begtrup G E, Gannett W, Yuzvinsky T D, et al. Nanoscale reversible mass transport for archival memory [J]. *Nano Lett*, 2009, **9**(5): 1835 - 1838.

[4] Goya G F, Berquo T S, Fonseca F C, et al. Static and dynamic magnetic properties of spherical magnetite nanoparticles [J]. *J Appl Phys*, 2003, **94**(5): 3520 - 3528.

[5] Kinnari P, Upadhyay R V, Mehta R V. Magnetic properties of Fe-Zn ferrite substituted ferrofluids [J]. *J Magn Magn Mater*, 2002, **252**(1/2): 35 - 38.

[6] Hamdeh H H, Ho J C. Magnetic properties of partially-inverted zinc ferrite aerogel powders [J]. *J Appl Phys*, 1997, **81**(4): 1851 - 1857.

[7] Hüseyin K, Abdülhadi B, Muhammet S T, et al. Cation distribution and magnetic properties of Zn doped $NiFe_2O_4$ nanoparticles synthesized by PEG-assisted hydrothermal route [J]. *J Alloy Compd*, 2009, **479**(1/2): 49 - 55.

[8] Pannunzio-Miner E V, De Paoli J M, Sanchez R D, et al. Crystal and magnetic structure and cation distribution of $Mn_{2-x}V_{1+x}O_4$ spinels ($x = 0$, 1/3 and 1) [J]. *Mater Res Bull*, 2009, **44**(7): 1586 - 1591.

[9] Suwalka O, Sharma R K, Sebastian V, et al. A study of nanosized Ni substituted Co-Zn ferrite prepared by coprecipitation [J]. *J Magn Magn Mater*, 2007, **313**(1): 198 - 203.

[10] Ma Ming, Zhang Yu, Yu Wei, et al. Preparation and characterization of magnetite nanoparticles coated by amino silane [J]. *Colloid Surface A*, 2003, **212**(2/3): 219 - 226.

[11] Srivastava C M, Shringi S N, Srivastava R G. Mössbauer study of relaxation phenomena in zinc-ferrous ferrites [J]. *Phys Rev B*, 1976, **14**(5): 2041 - 2050.

[12] Li Y T, Li Q, Wen M L, et al. Magnetic properties and local structure studies of Zn doped ferrites [J]. *J Electron Spectrosc Relat Phenom*, 2007, **160**(1/2/3): 1 - 6.

[13] Srivastava C M, Shringi S N, Srivastava R G, et al. Magnetic ordering and domain-wall relaxation in zinc-ferrous ferrites [J]. *Phys Rev B*, 1976, **14**(5): 2032 - 2040.

[14] Liou S H, Chien C L. Particle size dependent of the magnetic properties of ultrafine granular films. [J]. *J Appl Phys*, 1988, **63**(8): 4240 - 4242.

[15] Smit J, Wijn H P J. *Ferrites* [M]. New York: John Weily, 1959: 150.

锌铁氧体纳米颗粒的结构与磁性研究

张 毅 王 凯 任志艳 翟 亚

(东南大学物理系, 南京 211189)

摘要: 通过水热法制备了一系列具有不同锌含量的 $Zn_xFe_{3-x}O_4$ ($x = 0$, 0.15, 0.30, 0.40, 0.48, 0.60, 0.70) 纳米颗粒, 并利用透射电子显微镜、X 射线衍射仪、振动样品磁强计、超导量子干涉仪和穆斯堡尔谱仪对其进行研究. 所有样品均为尖晶石结构; 随着样品中锌含量的增加, 其晶格常数随之增加, 晶粒尺寸从 18 nm 减小到 9 nm. 在 5 K 和 293 K 时, $Zn_xFe_{3-x}O_4$ 纳米颗粒的饱和磁化强度首先随着 Zn 含量的增加而增大, 并在 $x = 0.4$ 时达到最大, 随后随着 Zn 含量的增加而减小. 室温下穆斯堡尔谱的测量结果表明:随着锌含量的增加, 谱线由较为标准的六线峰逐渐转变为双峰, 且在 $x = 0.60$ 时表现为明显的双峰结构, 而大块材料在 $x = 0.80$ 时才有类似结果. 饱和磁化强度和居里温度的测量结果表明,这种现象可能是由于样品中纳米颗粒表现出的超顺磁性导致的. 此外, 还讨论了离子分布对超精细磁场变化的影响, 并利用 Yafet-Kittel 模型对样品的磁性变化进行解释.

关键词: 磁性材料; 锌铁铁氧体; 穆斯堡尔谱; 磁性

中图分类号: O482